UCID- 20374

VAULT REFERENCE COPY

LINE: A Code Which Simulates Spectral Line Shapes for Fusion Reaction Products Generated by Various Speed Distributions

Dennis Slaughter
University of California
Lawrence Livermore National Laboratory
Livermore, CA 94550

March, 1985

Lawrence Livermore National Laboratory

This is an informal report intended primarily for internal or limited external distribution. The opinions and conclusions stated are those of the author and may or may not be those of the Laboratory.
Work performed under the auspices of the U.S. Department of Energy by the Lawrence Livermore National Laboratory under Contract W-7405-Eng-48.

DISCLAIMER

This document was prepared as an account of work sponsored by an agency of the United States Government. Neither the United States Government nor the University of California nor any of their employees, makes any warranty, express or implied, or assumes any legal liability or responsibility for the accuracy, completeness, or usefulness of any information, apparatus, product, or process disclosed, or represents that its use would not infringe privately owned rights. Reference herein to any specific commercial products, process, or service by trade name, trademark, manufacturer, or otherwise, does not necessarily constitute or imply its endorsement, recommendation, or favoring by the United States Government or the University of California. The views and opinions of authors expressed herein do not necessarily state or reflect those of the United States Government or the University of California, and shall not be used for advertising or product endorsement purposes.

Printed in the United States of America
Available from
National Technical Information Service
U.S. Department of Commerce
5285 Port Royal Road
Springfield, VA 22161
Price: Printed Copy $; Microfiche $4.50

Page Range	Domestic Price	Page Range	Domestic Price
001-025	$ 7.00	326-350	$ 26.50
026-050	8.50	351-375	28.00
051-075	10.00	376-400	29.50
076-100	11.50	401-426	31.00
101-125	13.00	427-450	32.50
126-150	14.50	451-475	34.00
151-175	16.00	476-500	35.50
176-200	17.50	501-525	37.00
201-225	19.00	526-550	38.50
226-250	20.50	551-575	40.00
251-275	22.00	576-600	41.50
276-300	23.50	601-up[1]	
301-325	25.00		

[1]Add 1.50 for each additional 25 page increment, or portion thereof from 601 pages up.

LINE: A Code Which Simulates Spectral Line Shapes for Fusion Reaction Products Generated by Various Speed Distributions

Dennis Slaughter
Lawrence Livermore National Laboratory
University of California
Livermore, CA 94550

ABSTRACT

A computer code is described which estimates the energy spectrum or "line-shape" for the charged particles and γ-rays produced by the fusion of low-z ions in a hot plasma. The simulation has several "built-in" ion velocity distributions characteristic of heated plasmas and it also accepts arbitrary speed and angular distributions although they must all be symmetric about the z-axis. An energy spectrum of one of the reaction products (ion, neutron, or γ-ray) is calculated at one angle with respect to the symmetry axis. The results are shown in tabular form, they are plotted graphically, and the moments of the spectrum to order ten are calculated both with respect to the origin and with respect to the mean.

Introduction

High temperature high density plasmas have substantial fusion rates among their low-z ions. Fusion reaction products are typically very energetic and may escape the plasma so that their energy and trajectory may be measured without perturbing the plasma. Energy spectrum measurements on fusion reaction products have been used in the past to determine the temperature of thermonuclear plasmas[1-9] from the doppler width of their spectral lines. These measurements have been based on the observation of fusion neutrons[1-9] as well as charged particles[10-16]. Some of the measurements have identified non-maxwellian ion speed distributions[17-19] by proper interpretation of the line shape and/or its location.

It has been proposed to determine the energy spectrum of confined fusion product α-particles in ignited D-T plasma by observing γ-rays or neutrons produced when they react with ions present in the plasma[20-21]. It may also be possible to determine the mean ion energy from the width of the γ-ray line produced by D-T fusion[22-23].

Interpretation of reaction product spectral data is based on the predicted "line-shape" in the energy spectrum of the particles observed. Predicted line shapes for neutron emission have been described for Maxwellian plasmas[1,24-27] and some non-maxwellian distributions[24-25]. While the fusion product

energy spectrum may be calculated semi-analytically for a Maxwellian ion speed distribution[24-27], a numerical integration procedure must be used for most other plausible speed distributions.

Fusion experiments operating now and those planned for the near future employ extensive heating with injected neutrals and absorbed rf power to elevate the energy of both ions and electrons. These processes commonly result in ion speed distributions which are non-maxwellian to a very significant extent. Maxwellian plasmas have become the exception in modern large scale fusion experiments. As a result, interpretation of reaction product spectral data requires that the expected line shape be established for each of the plausible ion speed distributions.

As plasma confinement and energy improves, reactions between fusion products and ions in the plasma should also be expected. These reactions may lead to additional spectral lines in the particle and γ-ray radiation leaving the plasma. Line shapes in these spectra may be helpful in determining the slowing down distribution of fusion products as they thermalize. It is the need to predict the line spectra of reaction products as a function of the angular and speed distribution of the reacting species which motivates the present simulation.

The computer simulation described below facilitates this process. In particular, it allows arbitrary speed and angular distributions for two reacting species and predicts the

observed energy spectrum of one of the reaction products. Reaction kinematics are calculated for non-relativistic ions and neutrons as well as for γ -rays. In each simulation the predicted spectra are calculated, displayed graphically, and all of the moments to order ten are calculated with respect to both the origin and the mean particle energy so that spectral shape due to different ion speed distributions may be compared quantitatively.

SPECTRUM CALCULATION

All of the simulations assume an axis of symmetry about which the velocity distributions of both reacting species are symmetric. This is the z-axis and the reaction product distribution will be symmetrical about it as a result of the assumption. The reaction is shown schematically in Figure 1. Spectral intensity is calculated at an angle θ_n relative to the symmetry (z) axis using the input angular and energy distributions for the reacting species. The result is reaction weighted by including the reaction cross section and its angular dependence in the simulation. Selection of a reaction of interest identifies the cross section to be used, the energy released in the reaction (Q), and the reaction product whose energy spectrum is to be estimated. It is assumed that all reactions are "two body" type and of the form:

$$m_1 + m_2 \rightarrow m_n + m_R \qquad (1)$$

where the reaction product of interest, m_n, may be a nucleon or photon but all others species must be classical non-relativistic particles with nonzero rest mass. Reactions

for which a line shape may be calculated are listed in Table I. The table also shows the reaction Q values used and references for the cross section data used.

TABLE I

REACTION LIST

Index	Reaction	Q(MeV) ref. 28	Product	σ ref.	Ang. dist reference
1	D(d,n)3He	3.267	n	29	24
2	D(d,p)T	4.032	p	29	24
3	T(d,n)4He	17.586	n	29	isotropic
4	3He(d,p)4He	18.351	p	29	isotropic
5	T(d,γ)5He	16.696	γ	29-33	isotropic
6	D(p,γ)3He	5.494	γ	34,35	isotropic
7	D(d,γ)4He	23.848	γ	36-38	36
8	T(p,γ)4He	19.814	γ	39	39
9	3He(d,γ)5He	16.388	γ	40-43	40-43
10	T(α,γ)7Li	2.467	γ	44,45	44,45
11	3He(α,γ)7Be	1.587	γ	46-48	47,48
12	6Li(α,γ)10B	4.461	γ	49-51	50
13	7Li(α,γ)11B	8.664	γ	52-54	isotropic
14	9Be(α,n)12C	5.704	n	55	55
15	9Be(α,n)12C*	1.265	n	55	isotropic
16	9Be(α,γ)14N	10.651	γ	55-58	isotropic
17	10B(α,n)13N	1.060	n	59-61	isotropic
18	10B(α,γ)14N	11.613	γ	62,63	isotropic
19	11B(α,n)14N	.157	n	64,65	isotropic
20	11B(α,γ)15N	10.992	γ	66,67	isotropic
21	12C(α,γ)16O	7.161	γ	68,69	isotropic
22	13C(α,n)16O	2.215	n	70,71	isotropic

In those cases where the cross section angular dependence is poorly known the reaction is assumed isotropic in the center-of-mass-coordinate-system (CMCS). In nearly all cases that assumption is a good one at the energies expected in a thermonuclear plasma. The result of the simulation is an estimation of $\phi(E_n,\theta_n)$ given by eq. 2 below.

$$\psi(E_n,\theta_n) = \int d^3\bar{v}_1 \int d^3\bar{v}_2 F_1(\bar{v}_1)F_2(\bar{v}_2)|\bar{v}_1-\bar{v}_2|\frac{d^2\sigma}{dEd\Omega_c}\frac{d\Omega_c}{d\Omega}K \qquad (2)$$

where

$F_1(V_1)$ and $F_2(V_2)$ are the normalized velocity distribution functions for the reacting species,

V_1 and V_2 are velocity vectors of the reacting species,

$d^2\sigma/dEd\Omega$ is the differential cross section in the CMCS

$d\Omega_c/d\Omega$ is the Jacobian to convert solid angles between the CMCS and the rest system,

$K(v_1,v_2,m_1,m_2,m_3,m_4,Q,E_n,\theta_n)$ is the kinematic kernel which determines the energy, E_n, of the reaction product at angle θ_n required by energy and momentum conservation.

An approximation to the desired result (2) is obtained by assuming that the speed and angular distributions are separable for both species. Then the functions F are described in terms of the input parameters by eq. 3 below.

$$F_i(V_i) = f(v_i)g(\mu_i)h(\phi_i) \qquad (3)$$

where $f(v)$ is the speed distribution, $g(\mu)$ the polar angle distribution, μ the cosine of the angle which the velocity vector makes with the z-axis, and $h(\phi)$ the azimuthal distribution is constant by assumption. In principle the integration (2) is carried out over six coordinates in velocity space. However, the reaction kinematics depend only on the

relative velocity of the reacting species so that one integration is eliminated trivially. The requirements of energy and momentum conservation in the kinematics eliminates one more of those coordinates when E_n and θ_n are fixed. The integral is then simplified to the form given in eq. 4 below.

$$\psi(E_n,\mu_n) = \int v_1^2 f_1(v_1)dv_1 \int v_2^2 f_2(v_2)dv_2 \int g_1(\mu_1)d\mu_1 \times \int g_2(\mu_2)d\mu_2 \int d\phi_2 v_R \frac{d^2\sigma}{dEd\Omega_c}\frac{d\Omega_c}{d\Omega} K \tag{4}$$

where K includes a delta function whose value is nonzero only when the velocity space coordinates of the reacting species satisfy the requirements of energy and momentum conservation for a reaction product at energy E_n and direction cosine μ_n. There are two methods of integration allowed: 1) a numerical procedure to evaluate the integral, and 2) monte carlo sampling of the input distribution functions with appropriate cross section weighting to determine the integral.

Numerical Integration of Eq. 4

In the first case, numerical integration, the angle and speed coordinates are divided up into a fixed number of equal increments and the integration is carried out using the trapezoidal rule. The number of increments in each coordinate is determined by the problem input. Evaluation of the integral for a given μ_n is repeated for each E_n in the result

table. The limits of integration for each coordinate must be determined by reaction kinematics so that a reaction product at energy E_n may be produced at angle θ_n relative to the z-axis. Since there is no closed form relation between the integration limits and the particle coordinates in velocity space it was considered simpler to work with equally spaced coordinate increments over a wide range. Each increment is checked for kinematically valid solutions and is skipped if none exist. Because of this, the user must be alert to the possibility that the choice of a small number of coordinate steps in the integration may lead to a very small number of parameter increments which contribute significantly to the actual integration. The importance of poor sampling is amplified by the cross section since it is very sensitive to the relative speed of the reacting species which, in turn, is very sensitive to the angular and speed coordinates.

Monte Carlo Integration of Eq. 4

Monte carlo integration relies on the random sampling of the input distribution functions which describe the velocity vectors of the reacting species. The probability of sampling any interval in the coordinate distribution is proportional to the integral over that interval. A large number of trials is carried out in which velocity vectors are assigned to the reacting species and the reaction product energy at the desired observation angle is calculated. An event weight is determined by calculating the differential cross section based on the

relative velocity of the reacting particles and the reaction product emission angle in the CMCS. The weight is accumulated in the appropriate energy bin of the reaction product energy spectrum. This result, with adequate trial statistics, should then simulate the expected energy spectrum of reaction products of interest. If the result spectrum is integrated over energy, the result corresponds to the expected differential reactivity (per unit energy per unit solid angle) at the observation angle.

SPEED DISTRIBUTIONS

The coordinate system and definition of angles used in the simulation are illustrated in Figure 1. Results of the simulation give the energy spectrum of reaction products observed at an angle θ with respect to the symmetry (z) axis. The angular distribution of species 1 and 2 must be given as a function of their respective direction cosines μ_1 and μ_2. Each reacting species is assigned a speed distribution. The distribution may be input in tabular form or may be calculated according to one of the "built-in" distributions using input parameters which characterize those generic distribution functions. Available distribution functions and their parameters are summarized below and in Table II .

The Maxwellian distribution is characteristic of plasmas in thermal equilibrium without high intensity heating. Its form is:

$$f(v) = c\, e^{-\frac{mv^2}{2T}} \qquad (5)$$

Neutral beam driven plasmas trap neutral atoms as well as diatomic and triatomic molecules at the beam energy Eb. Ionization of these species results in ions at the full beam energy as well as some at 1/2 and 1/3 the beam energy. The relative population in each group is a characteristic of the beam source. These ions are trapped and may be slowed by collisions or diffuse in velocity space by interaction with plasma fluctuations. The resulting speed distribution may be described crudely by one of the two following distribution functions. They are referred to here as the "three component Gaussian" and the "electron drag cooled" distribution. They are illustrated schematically in Figures 2 and 3.

Three component Gaussian[72]:

$$f(v) = c \sum_{j=1}^{3} \frac{b_j}{w_j} e^{-\left(\frac{v-v_j}{w_j}\right)^2} \tag{6}$$

where $$\frac{1}{2} m v_j^2 = E_b/j \tag{7}$$

Three component cooled distribution[72]:

$$f(E) = \frac{c}{E} \begin{bmatrix} b_1 \left(\frac{E}{E_b}\right)^{\alpha} & \text{for } \frac{1}{2} E_b < E < E_b \\ b_1 \left(\frac{E}{E_b}\right)^{\alpha} + b_2 \left(\frac{E}{\frac{1}{2}E_b}\right)^{\alpha} & \text{for } \frac{1}{3} E_b < E < \frac{1}{2}E_b \\ b_1 \left(\frac{E}{E_b}\right)^{\alpha} + b_2 \left(\frac{E}{\frac{1}{2}E_b}\right)^{\alpha} + b_3 \left(\frac{E}{\frac{1}{3}E_b}\right)^{\alpha} & \text{for } E_h < E < \frac{1}{3}E_b \\ 0 & \text{for } E < E_H \end{bmatrix} \tag{8}$$

Plasmas confined in a magnetic mirror topology may also be crudely parameterized according to the "mirror" distribution[72] which has the form:

$$f(v) = \begin{cases} 0 & \text{for } v<v_H \\ c(v-v_H)e^{-\left(\frac{v-v_o}{v_w}\right)^2} & \text{for } v>v_H \end{cases} \tag{9}$$

where

$$v_o = v_p - \frac{v_w^2}{2(v_p - v_H)} \tag{10}$$

Finally, very energetic reaction products which deposit their energy in the plasma during the process of thermalization will assume a continuum. One form is a reciprocal energy form given in eq. 11.

$$f(v) = \begin{cases} c\ v^{(\beta-2)} & \text{for } v<v_o \\ 0 & \text{for } v>v_o \end{cases} \tag{11}$$

Another plausible form of the expected continuum[73] is given in eq. 12 below.

$$f(v) = \begin{cases} 0 & \text{for } v>v_o \\ \frac{c}{v^3 + v_c^3} & \text{for } v<v_o \end{cases} \tag{12}$$

The speed distribution functions described above may be used during execution of the code, or another form may be supplied in tabular form as input. If one of the "built-in" distributions is used the code fills in the speed distribution table by calculating f(v) from the input parameters. Table II summarizes the available forms and the parameters needed to describe them completely. All input is normalized internally by the code.

TABLE II

SPEED DISTRIBUTIONS

Index	Name	Parameters
1	Maxwellian	m, T
2	3-component Gaussian[72]	E_b, b, W
3	3-component cooled[72]	Eb, b, α, E_h
4	1/E	β, v_0
5	Mirror	E_h, E_p, E_w
6	Alpha	E_c, E_a(max)
7	Tabular	VF, FV

KINEMATICS AND CROSS SECTIONS

Particle kinematics are described in their non-relativistic form. The relative speed between two reactants is given by eq. 13 and 14 below:

$$v_R = v_1 \sqrt{1 + \left(\frac{v_2}{v_1}\right)^2 - 2 \left(\frac{v_2}{v_1}\right) \mu_{12}} \qquad (13)$$

where

$$\mu_{12} = \mu_1\mu_2 + \sqrt{(1-\mu_1^2)(1-\mu_2^2)}\left[\cos\phi_1\cos\phi_2 + \sin\phi_1\sin\phi_2\right] \tag{14}$$

is the cosine of the angle between the velocity vectors of the reacting species, which are described in terms of their polar angles 198 relative to the z-axis, and their azimuthal angles ϕ relative to the x-axis.

The input cross section is allowed to have an anisotropic form in the CMCS. The probability of emission observed at angle θ_n in the rest system depends on the reaction product angle of emission in the CMCS. The cosine of the emission angle in the CMCS is given by eqs. 15 and 16 below:

$$\mu_{nc} = \frac{\mu_{n1} + \frac{m_2 v_2}{m_1 v_1}\mu_{n2}}{\sqrt{1 + \left(\frac{m_2 v_2}{m_1 v_1}\right)^2 + 2\frac{m_2 v_2}{m_1 v_1}\mu_{12}}} \tag{15}$$

where

$$\mu_{ni} = \mu_n\mu_i + \cos\phi_i\sqrt{(1-\mu_n^2)(1-\mu_i^2)} \tag{16}$$

are the cosines of the angle that the velocity vectors of the reacting species make with the observation vector.

The Jacobian which converts a solid angle in the CMCS to the corresponding angle in the rest frame is given[74] by eq. 17 and 18.

$$\frac{d\Omega_c}{d\Omega} = \frac{\sqrt{1 + \left(\frac{v_c}{v_n}\right)^2 - 2\frac{v_c}{v_n}\mu_{nc}}}{\mu_{nc} - \frac{v_c}{v_n}} \tag{17}$$

where

$$v_c = \sqrt{v_1^2 \left(\frac{m_1}{m_1+m_2}\right)^2 + v_2^2 \left(\frac{m_2}{m_1+m_2}\right)^2 + \frac{m_1 v_1 m_2 v_2}{(m_1+m_2)^2}\ \mu_{12}} \tag{18}$$

The Jacobian is nearly unity for most reacting species when their energies are much less than 1 MeV but may be important for reactions produced by some of the energetic reaction products.

Cross sections used here depend on the relative velocity of reacting species and the angle of the outgoing reaction product in the CMCS. While the cross section is very sensitive to reaction energy, this dependence may, to first order, be separated from the angular distribution. Eq. 4 is evaluated using the total reaction cross section multiplied by a weakly energy dependent angular distribution function, $g_s(E_c, \mu_c)$ according to eqs. 19 to 21 below.

$$\frac{d^2\sigma}{dE d\Omega_c}(E_c, \mu_c) = \frac{d\sigma}{dE}(E_c)\ g_s\ (E_c, \mu_c) \tag{19}$$

where

E_c is the total kinetic energy in the CMCS

$$g_s\,(E_c,\mu_c) = \frac{1 + \sum_{N=1}^{5} B_N\,(E_c)\,\mu_c^{\,N}}{4\pi\left[1 + \frac{B_2}{3} + \frac{B_4}{5}\right]} \tag{20}$$

$$B_N\,(E_c) = \sum_{j=0}^{5} b_{jN} E_c^{\,j} \tag{21}$$

μ_c is the cosine of the angle between the emission vector and the observation vector in the CMCS.

Thus the angular distribution factor $g_s(E,\mu)$ gives the probability per unit solid angle of emission along the observation vector in the CMCS and the coefficients B_i are weakly dependent on CMCS energy. Table I summarizes the values used and their sources. The cross sections, $\sigma(E_c)$, at energies below 500 keV are dominated by the coulomb barrier and are parameterized according to Peres[29] as follows:

$$\sigma(E_c) = \frac{A_s(E_c)}{E_c\left[e^{(B_c/\sqrt{E_c})} - 1\right]} \tag{22}$$

where

$$B_c = \pi Z_1 Z_2 \left(\frac{e^2}{\hbar c}\right) \sqrt{2m_e c^2} \tag{23}$$

and

$$A_s(E_c) = \frac{N_1 + E_c \left[N_2 + E_c \left[N_3 + \ldots\right]\right]}{1 + E_c \left[D_1 + E_c \left[D_2 + \ldots\right]\right]} \tag{24}$$

At higher energies the cross sections are parameterized according to eq. 25 below where the parameters are determined from a least squares fit of the fitting function to the available experimental data.

$$\sigma_c (E_c) = e^{\sum_{j=0}^{5} a_j (\ln E_c)^j} \tag{25}$$

The reaction product energy may then be calculated for non-relativistic nucleons from eqs. (26) - (30) below:

$$E_n = .5\ m_n\ V_n^2 \tag{26}$$

where

$$v_n = \frac{-B_n + \sqrt{B_n^2 - 4A_n c_n}}{2A_n} \tag{27}$$

and

$$A_n = \frac{1}{2} m_n \left(1 + \frac{m_n}{m_R}\right) \tag{28}$$

$$B_n = -\frac{m_n m_1}{m_R}\left(\mu_{n1} + \frac{m_2 v_2}{m_1 v_1}\mu_{n2}\right) \tag{29}$$

$$c_n = \frac{m_1 v_1 m_2 v_2}{m_R}\mu_{12} - Q - \frac{1}{2} m_2 v_2^2 \left(1 - \frac{m_2}{m_R}\right) - \frac{1}{2} m_1 v_1^2 \left(1 - \frac{m_1}{m_R}\right) \tag{30}$$

In the case of γ-ray emission the kinematics calculation is modified. The reaction product γ-ray has energy given by eqs. (31) -(34)

$$E_\gamma = \frac{-B_\gamma + \sqrt{B_\gamma^2 - 4A_\gamma c_\gamma}}{2A_\gamma} \tag{31}$$

where

$$A_\gamma = \frac{1}{2\, m_R c^2} \tag{32}$$

$$B_\gamma = 1 - \frac{m_1 v_1 \mu_{n1} + m_2 v_2 \mu_{n2}}{m_R c} \tag{33}$$

$$c_\gamma = c_n \tag{34}$$

RESULTS

An energy distribution function at observation angle θ_n is estimated for the reaction product ion, neutron, or γ-ray by evaluation of the reaction integral (4). The number of bins and their range in energy is set in the problem input. The accumulated cross section weighted data in each bin have the dimensions reactivity (cm^3/sec.) per unit energy (keV) per unit solid angle. The result spectra are displayed

graphically and in tabular form along with a regurgitation of the input parameters and input distribution functions. In order to assess the statistical significance of the calculated result during a monte carlo calculation a histogram is accumulated showing the number of trials which produced a whose kinematics produced a reaction product in each energy bin, regardless of cross section weight.

In addition, the moments of the result spectrum are calculated to order ten in order to quantitatively compare line shapes produced by different input distribution functions. Two forms of the moments are given. The first is with the origin as reference:

$$M_N = \frac{1}{M_0} \int_0^\infty E^N \psi(E)dE \tag{35}$$

where

$$M_0 = \int_0^\infty \psi(E)dE \tag{36}$$

The second uses the first moment (N=1, the mean value) from eq. 35 above as a reference.

$$M_N' = \frac{1}{M_0} \int_0^\infty \left(E - M_1\right)^N (E)dE \tag{37}$$

In practical application the integrals above are evaluated numerically and the procedure here is a simple trapezoidal rule approximation. The second set of moments provided in the

output results are obtained from eqs. 38-40 below.

$$M_N' = \frac{1}{M_o'} \sum_{j=1}^{NN-1} \left[\frac{1}{j+1} \left((E_{j+1} - M_1')^{j+1} - (E_j - M_1')^{j+1} \right) \right. \tag{38}$$

$$\left. \times \left(\psi_j + (E_j - M_1') \psi_j' \right) + \frac{1}{j+2} \left((E_{j+1} - M_1')^{j+2} - (E_j - M_1')^{j+2} \right) \psi_j' \right]$$

where

$$\psi_j' = \frac{\psi_{j+1} - \psi_j}{E_{j+1} - E_j} \tag{39}$$

$$M_o' = \frac{1}{2} \sum_{j=1}^{NN-1} (E_{j+1} - E_j) (\psi_{j+1} + \psi_j) \tag{40}$$

CONCLUSION

A computer simulation has been described which can predict the spectral line shape of fusion reaction products produced by energetic protons, deuterons, tritons, or α-particles in hot fusion plasma. Spectra are cross section weighted to correctly reflect the distortions in angular and energy distribution that will occur due to rapidly varying yield. The energy distribution of reacting species may take on any of the generic forms characteristic of modern driven plasmas or it may be given an arbitrary form. Results of the simulation include tabular and graphics displays as well as calculations of the spectral moments to order ten, with respect to the origin and the mean energy.

References

1) L. M. Goldman, R. W. Kilb, H. C. Pollock, "Measurement of Ion Energies in a θ-Pinch", Phys. Fluids 7, 1005 (1964).

2) S. P. Bogdanov, V. I. Volosov, "Measurements of the Ion Temperature in Plasmas from Neutron Radiation", Recent Advances in Plasma Diagnostics, Vol. 3, V. T. Tolok, Ed., Consultants Bureau, New York, 1971.

3) V. W. Slivinsky, H. G. Ahlstrom, K. G. Tirsell, J. Larsen, S. Glaros, G. Zimmerman, H. Shay, "Measurement of the Ion Temperature in Laser Driven Fusion", Phys. Rev. Lett. 35, 1083 (1975).

4) R. A. Lerche, L. W. Coleman, J. W. Houghton, D. R. Speck, E. K. Storm, "Laser Fusion Ion Temperatures Determined by Neutron Time of Flight Techniques", Appl. Phys. Lett. 31, 645 (1977).

5) F. Pecorella, M. Samuelli, A. Messina, C. Strangio, "Time and Space Resolved Neutron Measurements on a Dense Plasma Focus", Phys. Fluids 20, 675 (1977).

6) J. D. Strachan, P. Colestock, H. Eubank, L. Grisham, J. Hovey, G. Schilling, L. Stewart, W. Stodiek, R. Stooksberry, K. M. Young, "Measurement of the Neutron Spectra from Beam-Heated PLT Plasmas", Nature 279, 626 (1979).

7) K. Hubner, J. P. Rager, K. Steinmetz, "Space Resolved Investigations on the Plasma Focus Neutron Emission", Controlled Fusion and Plasma Physics, Vol. I, Moscow, September 14-19, 1981, p265.

8) D. R. Slaughter, H. S. Spracklen, R. Delvasto, "Time and Space Resolved Neutron Diagnostic Systems for Magnetically Confined Plasmas", Nuc. Inst. Meth. 215, 443 (1983).

9) W. A. Fisher, S. H. Chen, D. Gwinn, R. R. Parker, "A Fast Neutron Spectrometer for D-D Fusion Neutron Measurements at the Alcator C Tokamak", Nuc. Inst. Meth. 219, 179 (1984).

10) D. E. Nagle, W. E. Quinn, F. L. Ribe, W. B. Riesenfeld, "Velocity Spectrum of Protons and Tritons from the d-d Reaction in Scylla", Phys. Rev. 119, 857 (1960).

11) W. M. Jones, K. M. Young, A. C. L. Barnard, "Measurement of the Proton Energies from Sceptre III", J. Nucl. Energy, C3, 8 (1961).

12) R. E. Chrien, P. L. Colestock, H. P. Eubank, J. C. Hosea, D. Q. Hwang, J. D. Strachan, H. R. Thompson, Jr, "Observation of d-^{3}He Fusion Reactions in a Tokamak Plasma", Phys. Rev. Lett. 46, 535 (1981).

13) D. R. Welch, G. H. Miley, "Analysis of Doublet Proton Spectra", Bull. APS 28, 1152 (1983).

14) R. E. Chrien, R. Kaita, J. D. Strachan, "Observation of d(d,p)t Reactions in the Princeton Large Torus", Nuc. Fusion 23, 1399 (1983).

15) W. W. Heidbrink, "Fusion Reaction Spectra Produced by Anisotropic Fast Ions in the PLT Tokamak", PPPL-2079 (1984).

16) Jan S. Brzosko, H. Conrads, Jean Pierre Rager, B. V. Robouch, Karl Steinmetz, "Investigations of High Energy Deuterons in a Dense Plasma Focus Device by Means of Neutrons Emitted in the ^{7}Li+D Process", Nuc. Tech. Fusion 5, 209 (1984).

17) B. Rose, A. E. Taylor, E. Wood, "Measurement of the Neutron Spectrum From Zeta", Nature 181, 1630 (1958).

18) R. A. Coombe, B. A. Ward, "The Energy Spectra of the Neutrons from Zeta", Plasma Phys. 5, 273 (1963).

19) M. J. Bernstein, F. Hai, "Evidence for Nonthermonuclear Neutron Production in a Plasma Focus Discharge", Phys. Lett. 31A, 317 (1970).

20) D. E. Post, D. R. Mikkelsen, R. A. Hulse, L. D. Stewart, J. C. Weisheit, "Techniques for Measuring the Alpha Particle Distribution in Magnetically Confined Plasmas", J. Fusion Energy 1, 129 (1981).

21) D. R. Slaughter, "Nuclear Techniques for Determining the Spatial and Energy Distributions of Fast Confined Alpha Particles in Ignited DT Plasma", accepted for publication in Rev. Sci. Inst.

22) F. E. Cecil, David E. Newman, "Diagnostics of High Temperature Deuterium and Tritium Plasmas by Spectrometry of Radiative Capture Reactions", private communication.

23) S. S. Medley, H. Hendel, "Fusion Gamma Diagnostics for D-T and D-^{3}He Plasmas", PPPL-1950 (1982).

24) G. Lehner, F. Pohl, "Reaktionsneutronen als Hilfsmittel der Plasmadiagnostik", Z. Physik 207, 83 (1967).

25) M. M. R. Williams, "A Generalized Energy Exchange Kernel for Inelastic Neutron Scattering and Thermonuclear Reactions", J. Nuc. Energy 25, 489 (1971).

26) H. Brysk, "Fusion Neutron Energies and Spectra", Plasma Physics 15, 611 (1973).

27) H. Liskien, "The Particle Spectrum to be Expected from a D-T Plasma", Nuc. Sci. Eng. 71, 57 (1979).

28) C. Maples, G. W. Goth, J. Cerny, Nuclear Data 2, 429 (1966).

29) Asher Peres, J. Appl. Phys. 50, 5569 (1979).

30) Peter Batay Csorba, PhD Thesis, California Inst. Tech., 1975.

31) V. M. Bezotosnyi, Sov. J. Nucl. Phys. 10, 127 (1970).

32) W. Buss, Phys. Lett. 4, 198 (1963).

33) C. Rolfs, H. Truatvetter, Ann. Rev. Nucl. and Particle Sci., 115 (1978).

34) Griffiths, Can. J. Phys. 41, 724 (1963).

35) C. C. Chang, E. M. Diener, E. Ventura, Phys. Rev. Lett. 29, 307 (1972).

36) B. H. Flowers, F. Mandl, Proc. Roy. Soc. A206, 131 (1951).

37) W. E. Meyerfoff, W. Feldman, S. Gilbert, W. OConnell, Nuc. Phys. A131, 489 (1969).

38) J. M. Poutissou, W. DelBianco, Nuc. Phys. A199, 517 (1973).

39) S. Fiarman, W. E. Meyerhof, Nuc. Phys. A206, 1 (1973).

40) L. Kraus, M. Suffert, D. Magnac-Valette, Nuc. Phys. A109, 593 (1968).

41) W. DelBianco, F. Lemire, R. J. A. Levesque, J. M. Poutissou, Can. J. Phys. 46, 1585 (1968)

42) W. Buss, W. DelBianco, H. Waffler, B. Ziegler, Nuc. Phys. A112, 47 (1968).

43) H. T. King, W. E. Meyerhof, R. G. Hirko, Nuc. Phys. A178,337 (1972).

44) G. M. Griffiths, R. A. Morrow, P. J. Riley, J. B. Warren, Can. J. Phys. 39, 1397 (1961).

45) R. E. Brown, G. G. Olsen, R. F. Haglund, Jr., Nelson Jarmie, Phys. Rev. C16, 513 (1977).

46) J. L. Osborne, C. A. Barnes, R. W. Kavanaugh, R. M. Kremer, G. J. Mathews, J. L. Zyskind, Phys. Rev. Lett. 48, 1664 (1982).

47) K. Nagatoni, M. R. Dwarakanath, D. Ashery, Nuc. Phys. A128, 325 (1969).

48) C. E. Waltham, S. H. Chew, J. Lowe, J. M. Nelson, Nuc. Phys. A395, 119 (1983).

49) E. L. Sprenkel, J. W. Olness, R. E. Segel, Phys. Rev. Lett. 7, 174 (1961).

50) A. Auwarter, V. Meyer, Nuc. Phys. A242, 129 (1975).

51) P. D. Forsyth, H. T. Tu, W. F. Hornyak, Nuc. Phys. 82, 33 (1966).

52) G. A. Jones, C. M. P. Johnson, D. H. Wilkinson, Phil. Mag. 4, 796 (1959).

53) P. Paul, N. G. Puttaswamy, Phys. Rev. 164, 1332 (1967).

54) L. L. Green, G. A. Stephens, J. C. Willmott, Proc. Phys. Soc. 79, 1017 (1962).

55) F. Hinterberger, R. Schonhagen, P. VonRossen, B. Schuller, F. E. Blumenberg, P. D. Eversheim, R. Gorgen, Nuc. Phys. A308, 61 (1978).

56) J. B. Seaborn, G. E. Mitchel, N. R. Fletcher, R. H. Davis, Phys. Rev. 129, 2217 (1963).

57) J. H. Gibbons, R. L. Macklin, Phys. Rev. 137, B1508 (1965).

58) R. G. Miller, R. W. Kavanaugh, Nuc. Phys. 88, 492 (1966).

59) E. S. Shire, J. R. Wormald, G. Lindsay-Jones, A. Lunden, A. G. Stanley, Phil. Mag. 44, 41 (1953).

60) E. S. Shire, R. D. Edge, Phil. Mag. 46, 640 (1955).

61) L. Van der Zwan, K. W. Geiger, Nuc. Phys. A216, 188 (1973).

62) A. Gallmann, F. Hibou, P. Fintz, Nuc. Phys. A123, 27 (1969).

63) P. David, J. Debrus, H. Mommsen, A. Riccato, Nuc. Phys. A182, 234 (1972).

64) G. S. Mani, G. C. Dutt, Nuc. Phys. 78, 613 (1966).

65) L. Van der Zwan, K. W. Geiger, Nuc. Phys. A246, 93 (1975).

66) A. Degre, M. Schaeffer, G. Bonneaud, I. Linck, Nuc. Phys. A306, 77 (1978).

67) W. DelBianco, S. Kundu, J. Kim, Can. J. Phys. 55, 302 (1977).

68) P. Dyer, C. A. Barnes, Nuc. Phys. A233, 495 (1974).

69) T. R. Ophel, A. D. Frawley, P. B. Treacy, K. H. Bray, Nuc. Phys. A273, 397 (1976).

70) Davids, Nuc. Phys. A110, 619 (1968).

71) Bair, Phys. Rev. C7, 1356 (1973).

72) Dennis Slaughter, "Fusion Reactivities for Several Beam and Target Ion Distributions", J. Appl. Phys. 54, 1209 (1983).

73) D. E. Post, D. R. Mikkelsen, R. A. Hulse, L. D. Stewart, J. C. Weisheit, J. Fusion Energy 1, 129 (1981).

74) J. Monahan, "Kinematics of Neutron Producing Reactions", Fast Neutron Physics Part I, J. B. Marion, J. L. Fowler, Eds., Interscience, New York, 1960, p71.

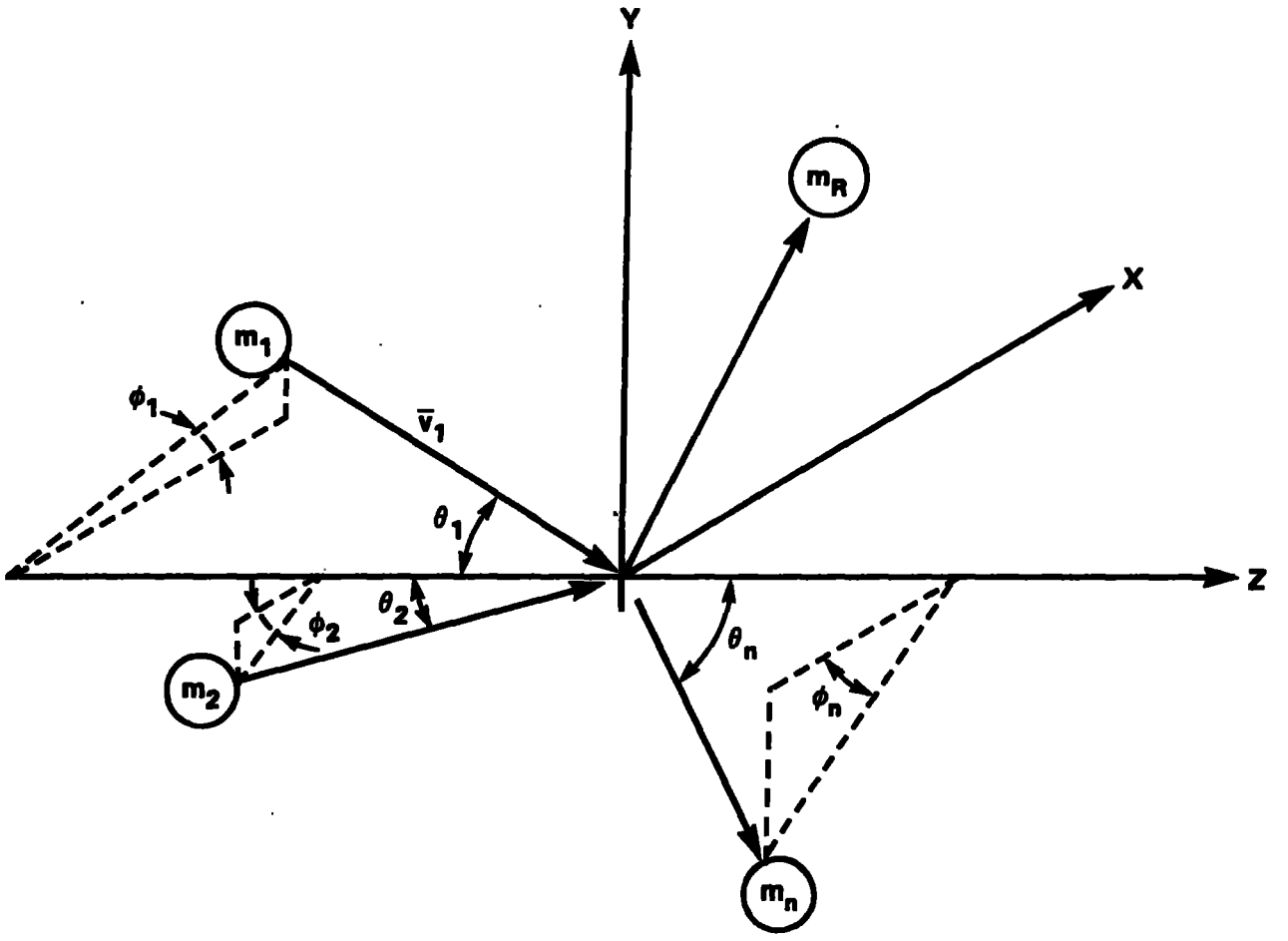

Fig. 1. Reaction geometry

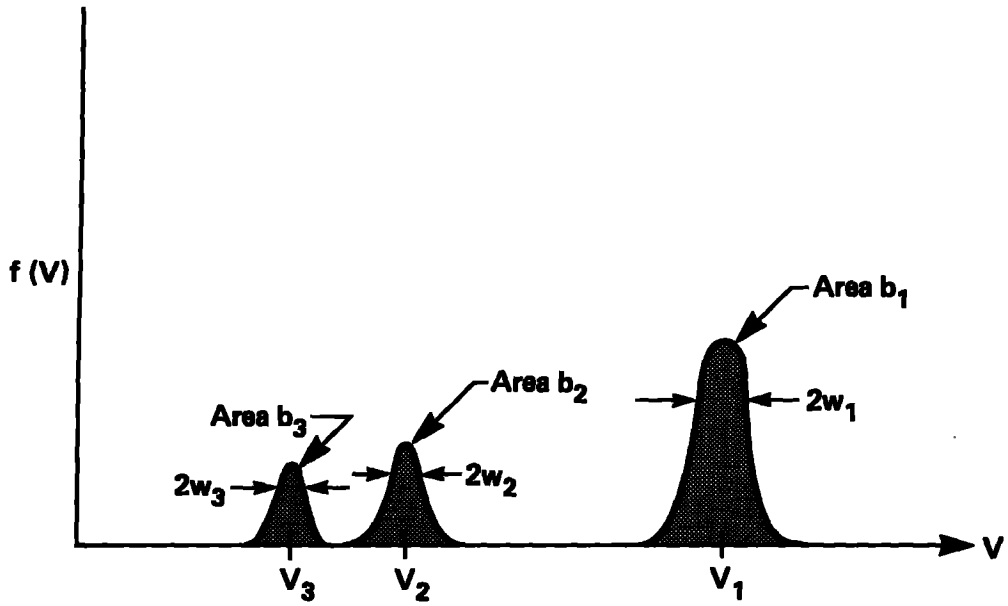

Fig. 2. Three component Gaussian speed distribution.

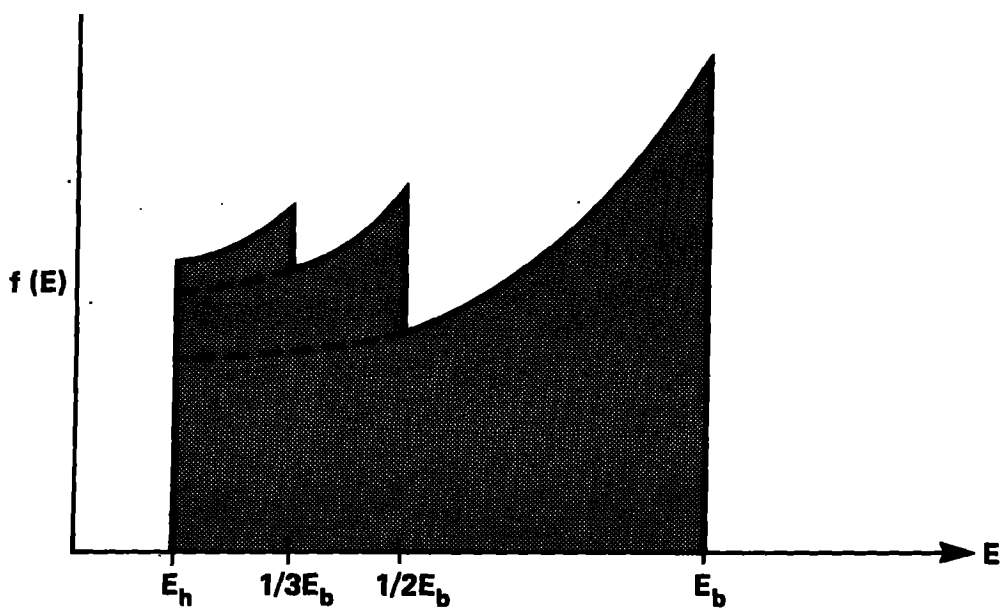

Fig. 3. Three component electron-drag-cooled speed distribution.

APPENDIX A

OPERATING MANUAL

The code described here runs on both the CDC 7600 and the Cray. All of the files including a library of Fortran sources (subroutine modules combined using LIB) and documentation are available in a .T directory. They may be obtained using XPORT as follows:

.826588:LINESHAPE:LINE	7600 controllee
.826588:LINESHAPE:LINECRAY	Cray controllee
.826588:LINESHAPE:LINESRC	7600 source
.826588:LINESHAPE:LINCRAYS	Cray source
.826588:LINESHAPE:LINEDOC	documentation file

Operation of the code is directed from the TTY by a set of COMMAND words and by input parameters. There is a full set of default values for the input parameters which may be modified or used "as-is". Input parameters may be supplied from the TTY or modified there, or they may be supplied in an input disc file. Execution is initiated as follows:

LINE (OUTPUT FILENAME) BOX ANN ID TV / t v

where

OUTPUT FILENAME= a printer file name containing the results and regurgitation of input parameters.

TV= an <u>optional</u> TMDS number.

In all cases an additional file is created and contains only the output spectrum for the problem. Its name is supplied with the INTEG or MONTE commands. Following the execute line above,

all further processing is directed by the command words supplied from the terminal and their arguments. A command word is required whenever the code sends an "OK:" prompt to the terminal.

COMMAND WORDS

One of the following COMMAND WORDS is required at the TTY whenever an "OK" prompt is sent. Accompanying arguments are indicated in parenthesis.

BINNER (#bins) (output filename) (input filename)

Reads previously generated spectrum results file and converts it to a new energy bin basis.

DATA (filename)

Read input parameters which are to be modified for the current problem from a disc file.

END (hardcopy)

Terminate execution and generate hardcopy fiche of the graphics output. If any argument is supplied then hardcopy fiche of the printer output will also be generated.

INTEG (result filename)

Solve the current problem by numerical integration using current values of input parameters.

HELP

Send a list of the command words to the TTY.

LIST (list name)

List the current value of all input parameters to the TTY. If no argument is given then all values are sent. If the name of one of the parameter lists below is supplied as an argument, then only that list is presented at the TTY.

MONTE (result filename)

Solve the current problem by monte carlo sampling of the input distributions using current input parameter values. Note: During a monte carlo evaluation the number of samples and the maximum time limit may be queried and changed as follows:

Type: NPART

to find their current values.

Type: NPART 10

to change the maximum number of samples to 10.

Type: NPART 10.

to change the maximum time limit to 10 seconds of CPU time.

PARAM

Change input parameter values in any of the lists defined below.

TIME (sec.)

Change the maximum time limit on CPU charges for the current problem.

TVOFF

Release the TMDS monitor.

TVON (monitor number)

Turn on TMDS to view graphics as they are generated.

PARAMETER LISTS

There are three parameter lists identified in a Fortran NAMELIST declaration. Input to these lists must be in NAMELIST format, i.e. a string of assignments of the form NAME=value (space delimited) with the string terminated in "$", but there is no constraint on the order of occurrence or on completeness of the input list. Only variables which are to be changed from their current (or default) values need to be supplied. The variable lists have names "A1", "A2", "S1" and their respective variable names, array dimensions, and default values are given below. Those corresponding to an array have their array dimensions given (without units) immediately following their name. Default values are given in parenthesis.

****

<u>LIST A1</u>

E1 =(20. keV)

Beam energy when species #1 is to be monoenergetic.

ENL =(2000. keV)

Energy of lowest bin in reaction product energy spectrum.

ENH =(3000. keV)

Energy of highest bin in reaction product energy spectrum.

ISPEED(2) = (1,1)

Index number defining speed distributions for species 1 and 2. Allowed values and use by the code are given below:

1 Maxwellian

2 Three component Gaussian

3 Electron drag cooled, three component distribution.

4 1/E distribution

5 Mirror

6 Alpha

7 Tabular input.

MODE = (0)

Index number defining special cases of the distribution function for species #1.

0 Monoenergetic, monodirectional beam whose axis is the symmetry axis.

1 Polyenergetic, monodirectional beam whose axis is the symmetry axis, but with speed distribution defined by F10 below.

2 Monoenergetic, axially symmetric distribution whose angular distribution is given by G10 below.

3 not used

4 Polyenergetic species with angular distribution symmetric about the z-axis.

MU1 = (1.)

Direction cosine of species #1 relative to z-axis. (Mode=1)

NBIN = (25)

Number of bins following BINNER command above.

NDEBUG = (0)

1 Turns on extra graphics to display monte carlo sampling of speed and angular distributions for debugging a problem.

NERRMAX = (20)

Maximum number of detected kinematic or integration errors following INTEG command before problem is terminated.

NMU1 = (3)

Number of integration steps in species #1 direction cosine.

NMU2 = (3)

Number of integration steps in species #2 direction cosine.

NN (100)

Number of bins in the output spectrum

NPART = (100)

Number of reaction trials following MONTE command.

NPHI1 = (3)

Number of integration steps in azimuth angle, species #1.

NPHI2 = (3)

Number of integration steps in azimuth angle, species #2.

NR = (1)

Index corresponding to problem reaction. Allowed values and their interpretation by the code are shown in Table I.

NV1 = (3)

Number of integration steps over speed distribution, species #1.

NV2 = (3)

Number of integration steps over speed distribution, species #2.

NVF1 = (100)

Number of entries in tabular speed distribution for species #1.

NVF2 = (100)

Number of entries in tabular speed distribution for species #2.

PHI1 = (0. rad)

Initial azimuth angle for species #1.

THETAN = (0. rad)

Angle at which reaction product is observed relative to z-axis.

TL = (60. sec.)

Maximum CPU time limit.

V1L = (1.)

Lower speed limit for species #1 in (keV/amu)**.5

V1H = (10.)

Upper speed limit for species #1 in (keV/amu)**.5

V2L =(1.)

Lower speed limit for species #2 in (keV/amu)**.5

V2H = (10.)

Upper speed limit for species #2 in (keV/amu)**.5

****

LIST A2

B(5,5) = (.13, .0047)

Energy dependent coefficients describing angular distribution of reaction product emission in the CMCS. They are used in calculating the cross section for emission at the desired observation angle according to eqs. 19 and 20:

$\sigma(E,\mu)=\sigma(E)*(1.+B(E)*\mu**2)$

where

B(E) = B(1) + B(2)*E + B(3)*E**2.....

EN(100)

Reaction product bin energies for output spectrum. NN entries.

F10(100)

Speed distribution function, $f(v_1)$, for species #1. NVF1 entries, each proportional to probability that particle of type 1 has speed VF1.

F20(100)

Speed distribution function, $f(v_2)$, for species #2. NVF2 entries, each proportional to probability that particle of type 2 has speed VF2.

G10(50) (1.,1.,.....)

Angular distribution, $g(\mu_1)$, for species #1. NMUG1 entries, each proportional to probability that direction cosine of particle of type 1 relative to z-axis has value MU10.

G20(50) (1.,1.,.....)

Angular distribution, $g(\mu_2)$, for species #2. NMUG2 entries, each proportional to the probability that direction cosine for particle of type 2 relative to z-axis has value MU20.

LABV1(5)

Five word label for speed distribution, species #1.

LABV2(5)

Five word label for speed distribution, species #2.

LABG1(5)

Five word label for angular distribution, species #1.

LABG2(5)

Five word label for angular distribution, species #2.

LABSIG(5)

Five word label for cross section used.

LABR(5)

Five word label for the reaction in the current problem.

MU10(50)

Direction cosines corresponding to angular distribution G10.

MU20(50)

Direction cosines corresponding to angular distribution G20.

NB (2)

Number of entries in B.

NMUG1 (21)

Number of entries in angular distribution G10.

NMUG2 (21)

Number of entries in angular distribution G20.

NG1SET (0)

MU10 and G10 are normally taken from their default values. Set this parameter = 1 if an input table for those parameters is to be used instead.

NG2SET (0)

MU20 and G20 are normally taken from their default values. Set this parameter = 1 if an input table for those parameters is to be used instead.

NSIGSET (0)

Cross sections are normally calculated internally according to the value of NR. Set this parameter = 1 if an input table is to be used.

NSIG (100)

Number of entries in the input cross section table SIG.

NVNSET (0)

Reaction product spectrum is normally displayed in equally spaced bins between the limits ENL and ENH. Set this parameter = 1 if an input table is to used to change the format of the output spectrum.

NV1SET (0)

Table F10 is normally calculated internally according to the value of ISPEED(1). Set this parameter =1 if in input table is to be used.

NV2SET (0)

Table F20 is normally calculated internally according to the value of ISPEED(2). Set this parameter =1 if an input table is to be used.

SIG(100)

Cross section values in cm**2.

VSIG(100)

Velocities corresponding to cross section entries in SIG, units of (keV/amu)**.5.

VF1(100)

Velocities corresponding to entries in speed distribution function F10, units of (keV/amu)**.5.

VF2(100)

Velocities corresponding to entries in speed distribution function F20, units of (keV/amu)**.5

****

<u>LIST S1</u>

ALPHA(2) = (2.,2.)

Exponent in electron drag cooled speed distribution. This is the parameter α in eq. 8. See figures 2 and 3.

BETA(2) = (-1.,-1.)

Exponent in the 1/E speed distribution. This is the parameter β in eq. 11.

BFRACT(3,2) =(.5,.4,.1 each col)

Relative intensity of components in three component speed distribution functions. This is the parameter b_j in eqs. 6 and 8. First component is full energy, last component 1/3 energy. See figures 2 and 3.

EAMAX(2) = (3500., 3500. keV)

Maximum particle energy in the 1/E or alpha distribution. This is the energy corresponding to the particle velocity v_0 in eqs. 11 and 12.

EB(2) =(20.,20. keV)

Full energy of beams in three component speed distributions. This is the parameter E_b in eqs. 7, and 8.

EC(2) = (100., 100. keV)

Critical energy in alpha distribution. This is the energy corresponding to the critical particle velocity v_c in eq. 12.

EHOLE(2) = (2.,2. keV)

Lower limit of particle energy in three component speed distribution function. This is the parameter E_h in eq. 8 and is the energy corresponding to the particle cutoff velocity v_h in eqs. 9 and 10.

EP(2) = (12., 12. keV)

Peak energy parameter in mirror distribution. This is the energy corresponding to particle velocity v_p in eq. 10.

EW(2) = (1., 1. keV)

Peak width parameter in in mirror distribution. This is the energy corresponding to particle velocity width parameter v_w in eqs. 9 and 10.

G(2) = (.0425,.0425)

Dispersion parameter in three component Gaussian speed distribution. It is used to calculate the width w_j in eq. 6 according to

$$w_j = g \times v_j$$

TEMP(2) (10.,10. keV)

Temperature parameter for Maxwellian speed distribution.

EXAMPLE PROBLEM

```
LINEG OUT BOX 072 SLAUGHTER 1737 / 5 1
OK:       MONTE TEST1
A1:       NPART=50000 V1L=3. V1H=30. MODE=1 ISPEED(1)=2$
LABEL:    TEST PROBLEM
S1:       EB(1)=50. (BFRACT(I,1),I=1,3)=.8 .1 .1$
S1:       TEMP(2)=50.$
OK:       END OUT
ALL DONE
```

```
1  INPUT:        MONTE     TEST1
  TIME STAMP:   11:29:46  01/29/85  U
 THIS IS A *****  MONTE CARLO CALCULATION ***
 TEST PROBLEM

     *** POLY ENERGETIC BEAM PROBLEM ***


INPUT PARAMETERS:

     PHI1=        0.          MU1=       1.00E+00  V1=        0.          E1=        2.00E+01
     NPHI1=              3   NMU1=              3  NVF1=           100  NR=               1
     V1L=         3.00E+00    V1H=       3.00E+01  V2L=       1.00E+00  V2H=       1.00E+01
     NPHI2=              3   NMU2=              3  NVF2=           100  MODE=             1
     ENL=         2.00E+03    ENH=       3.00E+03  NN=             100  NBIN=            25
     EN0=         0.          THETAN=    0.        NPART=        50000  TL=        6.00E+01
     NV1=                3   NV2=               3  NDEBUG=           0  NERRMAX=         20

 SPEED DISTRIBUTION FOR SPECIES #1 NVSET=    0
```

I	V	F	I	V	F	I	V	F
1	3.0000E+00	1.6510E-10	35	1.2273E+01	3.1745E-65	69	2.1545E+01	0.
2	3.2727E+00	1.0371E-06	36	1.2545E+01	3.3114E-72	70	2.1818E+01	0.
3	3.5455E+00	5.4296E-04	37	1.2818E+01	1.5144E-79	71	2.2091E+01	0.
4	3.8182E+00	2.3743E-02	38	1.3091E+01	3.0367E-87	72	2.2364E+01	0.
5	4.0909E+00	8.6871E-02	39	1.3364E+01	2.6700E-95	73	2.2636E+01	0.
6	4.3636E+00	2.7533E-02	40	1.3636E+01	1.0294-103	74	2.2909E+01	0.
7	4.6364E+00	2.1777E-02	41	1.3909E+01	1.7403-112	75	2.3182E+01	0.
8	4.9091E+00	9.3310E-02	42	1.4182E+01	1.2902-121	76	2.3455E+01	0.
9	5.1818E+00	7.9006E-02	43	1.4455E+01	4.1945-131	77	2.3727E+01	0.
10	5.4545E+00	1.2813E-02	44	1.4727E+01	5.9802-141	78	2.4000E+01	0.
11	5.7273E+00	4.3400E-04	45	1.5000E+01	3.7392-151	79	2.4273E+01	0.
12	6.0000E+00	1.5098E-03	46	1.5273E+01	1.0253-161	80	2.4545E+01	0.
13	6.2727E+00	2.7715E-02	47	1.5545E+01	1.2331-172	81	2.4818E+01	0.
14	6.5455E+00	2.2277E-01	48	1.5818E+01	6.5043-184	82	2.5091E+01	0.
15	6.8182E+00	7.8309E-01	49	1.6091E+01	1.5047-195	83	2.5364E+01	0.
16	7.0909E+00	1.2042E+00	50	1.6364E+01	1.5268-207	84	2.5636E+01	0.
17	7.3636E+00	8.1024E-01	51	1.6636E+01	6.7950-220	85	2.5909E+01	0.
18	7.6364E+00	2.3860E-01	52	1.6909E+01	1.3264-232	86	2.6182E+01	0.
19	7.9091E+00	3.0755E-02	53	1.7182E+01	1.1357-245	87	2.6455E+01	0.
20	8.1818E+00	1.7357E-03	54	1.7455E+01	4.2654-259	88	2.6727E+01	0.
21	8.4545E+00	4.2892E-05	55	1.7727E+01	7.0269-273	89	2.7000E+01	0.
22	8.7273E+00	4.6419E-07	56	1.8000E+01	5.0778-287	90	2.7273E+01	0.
23	9.0000E+00	2.2003E-09	57	1.8273E+01	0.	91	2.7545E+01	0.
24	9.2727E+00	4.5688E-12	58	1.8545E+01	0.	92	2.7818E+01	0.
25	9.5455E+00	4.1561E-15	59	1.8818E+01	0.	93	2.8091E+01	0.
26	9.8182E+00	1.6565E-18	60	1.9091E+01	0.	94	2.8364E+01	0.
27	1.0091E+01	2.8929E-22	61	1.9364E+01	0.	95	2.8636E+01	0.
28	1.0364E+01	2.2139E-26	62	1.9636E+01	0.	96	2.8909E+01	0.
29	1.0636E+01	7.4252E-31	63	1.9909E+01	0.	97	2.9182E+01	0.
30	1.0909E+01	1.0915E-35	64	2.0182E+01	0.	98	2.9455E+01	0.
31	1.1182E+01	7.0322E-41	65	2.0455E+01	0.	99	2.9727E+01	0.
32	1.1455E+01	1.9860E-46	66	2.0727E+01	0.	100	3.0000E+01	0.
33	1.1727E+01	2.4586E-52	67	2.1000E+01	0.	101	1.6510E-10	0.
34	1.2000E+01	1.3343E-58	68	2.1273E+01	0.	102	1.0371E-06	0.

```
   3-COMPON  ENT GAUS
     BEAM ENERGY=    5.00E+01  FRACTIONS=    8.00E-01    1.00E-01    1.00E-01
     G=    4.25E-02  ALPHA=    2.00E+00
```

ISPEED= 2
MEAN ENERGY= 4.775E+01

SPEED DISTRIBUTION FOR SPECIES #2 NVSET= 0

I	V	F	I	V	F	I	V	F
1	1.0000E+00	8.4962E-03	35	4.0909E+00	1.0380E-01	69	7.1818E+00	1.5936E-01
2	1.0909E+00	1.0073E-02	36	4.1818E+00	1.0684E-01	70	7.2727E+00	1.5918E-01
3	1.1818E+00	1.1773E-02	37	4.2727E+00	1.0984E-01	71	7.3636E+00	1.5890E-01
4	1.2727E+00	1.3593E-02	38	4.3636E+00	1.1278E-01	72	7.4545E+00	1.5852E-01
5	1.3636E+00	1.5529E-02	39	4.4545E+00	1.1565E-01	73	7.5455E+00	1.5804E-01
6	1.4545E+00	1.7579E-02	40	4.5455E+00	1.1847E-01	74	7.6364E+00	1.5746E-01
7	1.5455E+00	1.9737E-02	41	4.6364E+00	1.2121E-01	75	7.7273E+00	1.5679E-01
8	1.6364E+00	2.1999E-02	42	4.7273E+00	1.2389E-01	76	7.8182E+00	1.5603E-01
9	1.7273E+00	2.4362E-02	43	4.8182E+00	1.2648E-01	77	7.9091E+00	1.5518E-01
10	1.8182E+00	2.6821E-02	44	4.9091E+00	1.2900E-01	78	8.0000E+00	1.5424E-01
11	1.9091E+00	2.9370E-02	45	5.0000E+00	1.3143E-01	79	8.0909E+00	1.5321E-01
12	2.0000E+00	3.2006E-02	46	5.0909E+00	1.3378E-01	80	8.1818E+00	1.5211E-01
13	2.0909E+00	3.4722E-02	47	5.1818E+00	1.3603E-01	81	8.2727E+00	1.5092E-01
14	2.1818E+00	3.7514E-02	48	5.2727E+00	1.3820E-01	82	8.3636E+00	1.4966E-01
15	2.2727E+00	4.0377E-02	49	5.3636E+00	1.4026E-01	83	8.4545E+00	1.4833E-01
16	2.3636E+00	4.3306E-02	50	5.4545E+00	1.4223E-01	84	8.5455E+00	1.4692E-01
17	2.4545E+00	4.6293E-02	51	5.5455E+00	1.4410E-01	85	8.6364E+00	1.4545E-01
18	2.5455E+00	4.9336E-02	52	5.6364E+00	1.4587E-01	86	8.7273E+00	1.4391E-01
19	2.6364E+00	5.2426E-02	53	5.7273E+00	1.4753E-01	87	8.8182E+00	1.4231E-01
20	2.7273E+00	5.5560E-02	54	5.8182E+00	1.4909E-01	88	8.9091E+00	1.4066E-01
21	2.8182E+00	5.8730E-02	55	5.9091E+00	1.5054E-01	89	9.0000E+00	1.3894E-01
22	2.9091E+00	6.1932E-02	56	6.0000E+00	1.5189E-01	90	9.0909E+00	1.3718E-01
23	3.0000E+00	6.5160E-02	57	6.0909E+00	1.5312E-01	91	9.1818E+00	1.3536E-01
24	3.0909E+00	6.8407E-02	58	6.1818E+00	1.5424E-01	92	9.2727E+00	1.3350E-01
25	3.1818E+00	7.1668E-02	59	6.2727E+00	1.5526E-01	93	9.3636E+00	1.3159E-01
26	3.2727E+00	7.4937E-02	60	6.3636E+00	1.5616E-01	94	9.4545E+00	1.2965E-01
27	3.3636E+00	7.8209E-02	61	6.4545E+00	1.5696E-01	95	9.5455E+00	1.2767E-01
28	3.4545E+00	8.1477E-02	62	6.5455E+00	1.5764E-01	96	9.6364E+00	1.2565E-01
29	3.5455E+00	8.4736E-02	63	6.6364E+00	1.5821E-01	97	9.7273E+00	1.2360E-01
30	3.6364E+00	8.7981E-02	64	6.7273E+00	1.5867E-01	98	9.8182E+00	1.2153E-01
31	3.7273E+00	9.1206E-02	65	6.8182E+00	1.5902E-01	99	9.9091E+00	1.1943E-01
32	3.8182E+00	9.4405E-02	66	6.9091E+00	1.5927E-01	100	1.0000E+01	1.1731E-01
33	3.9091E+00	9.7573E-02	67	7.0000E+00	1.5940E-01	101	8.4962E-03	0.
34	4.0000E+00	1.0071E-01	68	7.0909E+00	1.5943E-01	102	1.0073E-02	0.

MAXWELL

TEMP= 5.00E+01 KEV
ISPEED= 1
MEAN ENERGY= 4.589E+01

ANGULAR DISTRIBUTION FOR SPECIES #2 NGSET= 0

I	MU	G	I	MU	G	I	MU	G
1	-1.0000E+00	5.0000E-01	8	-3.0000E-01	5.0000E-01	15	4.0000E-01	5.0000E-01
2	-9.0000E-01	5.0000E-01	9	-2.0000E-01	5.0000E-01	16	5.0000E-01	5.0000E-01
3	-8.0000E-01	5.0000E-01	10	-1.0000E-01	5.0000E-01	17	6.0000E-01	5.0000E-01
4	-7.0000E-01	5.0000E-01	11	0.	5.0000E-01	18	7.0000E-01	5.0000E-01
5	-6.0000E-01	5.0000E-01	12	1.0000E-01	5.0000E-01	19	8.0000E-01	5.0000E-01
6	-5.0000E-01	5.0000E-01	13	2.0000E-01	5.0000E-01	20	9.0000E-01	5.0000E-01
7	-4.0000E-01	5.0000E-01	14	3.0000E-01	5.0000E-01	21	1.0000E+00	5.0000E-01

CONSTANT

CROSS SECTION AS FUNCTION OF RELATIVE SPEED,NSIGSET= 0

I	V	SIGMA	I	V	SIGMA	I	V	SIGMA
1	1.7321E+00	2.5629E-34	35	5.0914E+00	6.6341E-28	69	1.4966E+01	2.7187E-26
2	1.7879E+00	5.3548E-34	36	5.2554E+00	8.1801E-28	70	1.5448E+01	2.8250E-26
3	1.8455E+00	1.0912E-33	37	5.4247E+00	1.0002E-27	71	1.5946E+01	2.9285E-26
4	1.9049E+00	2.1705E-33	38	5.5995E+00	1.2129E-27	72	1.6460E+01	3.0289E-26
5	1.9663E+00	4.2174E-33	39	5.7799E+00	1.4593E-27	73	1.6990E+01	3.1259E-26
6	2.0297E+00	8.0107E-33	40	5.9662E+00	1.7424E-27	74	1.7538E+01	3.2192E-26
7	2.0951E+00	1.4885E-32	41	6.1584E+00	2.0651E-27	75	1.8103E+01	3.3088E-26
8	2.1626E+00	2.7074E-32	42	6.3569E+00	2.4300E-27	76	1.8686E+01	3.3943E-26
9	2.2322E+00	4.8239E-32	43	6.5617E+00	2.8397E-27	77	1.9288E+01	3.4756E-26
10	2.3042E+00	8.4247E-32	44	6.7731E+00	3.2963E-27	78	1.9909E+01	3.5526E-26
11	2.3784E+00	1.4431E-31	45	6.9913E+00	3.8015E-27	79	2.0551E+01	3.6253E-26
12	2.4551E+00	2.4261E-31	46	7.2166E+00	4.3569E-27	80	2.1213E+01	3.6934E-26
13	2.5342E+00	4.0050E-31	47	7.4491E+00	4.9632E-27	81	2.1897E+01	3.7570E-26
14	2.6158E+00	6.4961E-31	48	7.6892E+00	5.6210E-27	82	2.2602E+01	3.8160E-26
15	2.7001E+00	1.0358E-30	49	7.9369E+00	6.3301E-27	83	2.3330E+01	3.8703E-26
16	2.7871E+00	1.6247E-30	50	8.1926E+00	7.0899E-27	84	2.4082E+01	3.9201E-26
17	2.8769E+00	2.5077E-30	51	8.4566E+00	7.8992E-27	85	2.4858E+01	3.9652E-26
18	2.9696E+00	3.8111E-30	52	8.7291E+00	8.7564E-27	86	2.5659E+01	4.0057E-26
19	3.0653E+00	5.7055E-30	53	9.0104E+00	9.6591E-27	87	2.6486E+01	4.0417E-26
20	3.1640E+00	8.4183E-30	54	9.3007E+00	1.0605E-26	88	2.7339E+01	4.0731E-26
21	3.2660E+00	1.2247E-29	55	9.6004E+00	1.1590E-26	89	2.8220E+01	4.1001E-26
22	3.3712E+00	1.7575E-29	56	9.9097E+00	1.2612E-26	90	2.9129E+01	4.1226E-26
23	3.4798E+00	2.4890E-29	57	1.0229E+01	1.3666E-26	91	3.0068E+01	4.1408E-26
24	3.5920E+00	3.4801E-29	58	1.0559E+01	1.4748E-26	92	3.1037E+01	4.1547E-26
25	3.7077E+00	4.8058E-29	59	1.0899E+01	1.5854E-26	93	3.2037E+01	4.1646E-26
26	3.8272E+00	6.5572E-29	60	1.1250E+01	1.6979E-26	94	3.3069E+01	4.1701E-26
27	3.9505E+00	8.8433E-29	61	1.1612E+01	1.8119E-26	95	3.4136E+01	4.1717E-26
28	4.0778E+00	1.1793E-28	62	1.1987E+01	1.9267E-26	96	3.5236E+01	4.1694E-26
29	4.2092E+00	1.5555E-28	63	1.2373E+01	2.0421E-26	97	3.6370E+01	4.1633E-26
30	4.3448E+00	2.0301E-28	64	1.2772E+01	2.1576E-26	98	3.7542E+01	4.1535E-26
31	4.4848E+00	2.6225E-28	65	1.3183E+01	2.2724E-26	99	3.8751E+01	4.1401E-26
32	4.6293E+00	3.3544E-28	66	1.3608E+01	2.3864E-26	100	4.0000E+01	4.1232E-26
33	4.7785E+00	4.2494E-28	67	1.4046E+01	2.4990E-26	101	2.5629E-34	0.
34	4.9324E+00	5.3335E-28	68	1.4499E+01	2.6099E-26	102	5.3548E-34	1.3000E-01

CROSS SECTION CMCS ANGULAR DIST COEFFICIENTS

1.30E-01 4.70E-03

1 MONTE CARLO RESULTS ARE PRINTED IN FILE: TEST1 TIME STAMP:11:29:46 01/29/85 U
D(D,N)^HE
TEST PROBLEM

RESULTS OF MONTECARLO SIMULATION FOR 50000 (3.20E+01 SEC) PARTICLES FROM REACTION # 0 (D,N)^HE
DISTRIBUTION OVER 100 BINS FROM 2.00E+03 TO 3.00E+03 KEV
M1= 2.0 M2= 2.0 MN= 1.0 MR= 3.0 Q= 3.27E+03
MODE= 1

I	EN	NO.	PSI	+/-
1	2.000E+03	0.	0.	0.
2	2.010E+03	0.	0.	0.
3	2.020E+03	0.	0.	0.
4	2.030E+03	0.	0.	0.
5	2.040E+03	0.	0.	0.
6	2.051E+03	0.	0.	0.
7	2.061E+03	0.	0.	0.
8	2.071E+03	0.	0.	0.
9	2.081E+03	0.	0.	0.
10	2.091E+03	0.	0.	0.
11	2.101E+03	0.	0.	0.
12	2.111E+03	0.	0.	0.
13	2.121E+03	0.	0.	0.
14	2.131E+03	0.	0.	0.
15	2.141E+03	0.	0.	0.
16	2.152E+03	0.	0.	0.
17	2.162E+03	0.	0.	0.
18	2.172E+03	0.	0.	0.
19	2.182E+03	0.	0.	0.
20	2.192E+03	0.	0.	0.
21	2.202E+03	0.	0.	0.
22	2.212E+03	0.	0.	0.
23	2.222E+03	0.	0.	0.
24	2.232E+03	0.	0.	0.
25	2.242E+03	0.	0.	0.
26	2.253E+03	0.	0.	0.
27	2.263E+03	0.	0.	0.
28	2.273E+03	0.	0.	0.
29	2.283E+03	0.	0.	0.
30	2.293E+03	0.	0.	0.
31	2.303E+03	0.	0.	0.
32	2.313E+03	0.	0.	0.
33	2.323E+03	0.	0.	0.
34	2.333E+03	0.	0.	0.
35	2.343E+03	2.	2.829E-24	2.001E-24
36	2.354E+03	9.	1.143E-23	3.809E-24
37	2.364E+03	12.	1.504E-23	4.340E-24
38	2.374E+03	12.	1.380E-23	3.983E-24
39	2.384E+03	21.	2.631E-23	6.624E-24
40	2.394E+03	19.	2.296E-23	5.267E-24
41	2.404E+03	29.	3.587E-23	6.661E-24
42	2.414E+03	31.	3.648E-23	6.553E-24
43	2.424E+03	41.	4.660E-23	6.967E-24
44	2.434E+03	52.	5.935E-23	8.230E-24
45	2.444E+03	62.	6.808E-23	8.646E-24
46	2.455E+03	82.	1.036E-22	1.143E-23
47	2.465E+03	100.	1.547E-22	1.489E-23
48	2.475E+03	153.	2.134E-22	1.725E-23
49	2.485E+03	218.	3.486E-22	2.361E-23

50	2.495E+03	233.	3.847E-22	2.520E-23
51	2.505E+03	335.	5.443E-22	2.974E-23
52	2.515E+03	438.	7.357E-22	3.515E-23
53	2.525E+03	444.	7.359E-22	3.492E-23
54	2.535E+03	562.	9.167E-22	3.867E-23
55	2.545E+03	627.	1.023E-21	4.087E-23
56	2.556E+03	720.	1.129E-21	4.206E-23
57	2.566E+03	792.	1.235E-21	4.390E-23
58	2.576E+03	869.	1.294E-21	4.390E-23
59	2.586E+03	866.	1.252E-21	4.253E-23
60	2.596E+03	993.	1.326E-21	4.206E-23
61	2.606E+03	1095.	1.390E-21	4.201E-23
62	2.616E+03	1125.	1.361E-21	4.056E-23
63	2.626E+03	1241.	1.413E-21	4.011E-23
64	2.636E+03	1302.	1.424E-21	3.947E-23
65	2.646E+03	1358.	1.386E-21	3.760E-23
66	2.657E+03	1340.	1.313E-21	3.588E-23
67	2.667E+03	1398.	1.258E-21	3.364E-23
68	2.677E+03	1366.	1.154E-21	3.122E-23
69	2.687E+03	1446.	1.131E-21	2.974E-23
70	2.697E+03	1425.	1.083E-21	2.868E-23
71	2.707E+03	1430.	9.761E-22	2.581E-23
72	2.717E+03	1507.	9.407E-22	2.423E-23
73	2.727E+03	1438.	8.182E-22	2.158E-23
74	2.737E+03	1493.	7.671E-22	1.985E-23
75	2.747E+03	1380.	6.814E-22	1.834E-23
76	2.758E+03	1343.	6.006E-22	1.639E-23
77	2.768E+03	1405.	5.696E-22	1.520E-23
78	2.778E+03	1343.	5.008E-22	1.366E-23
79	2.788E+03	1339.	4.445E-22	1.215E-23
80	2.798E+03	1264.	3.775E-22	1.062E-23
81	2.808E+03	1285.	3.535E-22	9.861E-24
82	2.818E+03	1174.	3.139E-22	9.160E-24
83	2.828E+03	1117.	2.633E-22	7.879E-24
84	2.838E+03	1106.	2.240E-22	6.734E-24
85	2.848E+03	1036.	2.025E-22	6.290E-24
86	2.859E+03	925.	1.666E-22	5.477E-24
87	2.869E+03	893.	1.368E-22	4.576E-24
88	2.879E+03	828.	1.211E-22	4.209E-24
89	2.889E+03	823.	1.124E-22	3.917E-24
90	2.899E+03	659.	7.731E-23	3.012E-24
91	2.909E+03	653.	6.935E-23	2.714E-24
92	2.919E+03	646.	6.702E-23	2.637E-24
93	2.929E+03	552.	4.712E-23	2.006E-24
94	2.939E+03	509.	3.845E-23	1.704E-24
95	2.949E+03	466.	3.014E-23	1.396E-24
96	2.960E+03	422.	2.331E-23	1.135E-24
97	2.970E+03	372.	1.873E-23	9.713E-25
98	2.980E+03	300.	1.008E-23	6.200E-25
99	2.990E+03	278.	8.773E-24	5.262E-25
100	3.000E+03	1180.	1.770E-23	5.154E-25

1 RESULT TABLE AREAS: 3.40E-19 WEIGHTED 5.00E+04 UNWEIGHTED

FWHM= 2.30E+02 0.

FWTM= 4.05E+02 0.

XXXXXXXXXXX MOMENTS XXXXXXXXX

M	SIGMA-WEIGHTED MOMENT	SIGMA-WEIGHTED ROOT	NON-WEIGHTED MOMENT	NON-WEIGHTED ROOT
1	2.6409E+03	0.	2.7300E+03	0.
2	6.9841E+06	2.6427E+03	7.4690E+06	2.7330E+03
3	1.8496E+10	2.6444E+03	2.0478E+10	2.7357E+03
4	4.9050E+13	2.6464E+03	5.6268E+13	2.7388E+03
5	1.3026E+17	2.6483E+03	1.5493E+17	2.7418E+03
6	3.4646E+20	2.6502E+03	4.2762E+20	2.7447E+03
7	9.2275E+23	2.6520E+03	1.1821E+24	2.7476E+03
8	2.4613E+27	2.6540E+03	3.2756E+27	2.7505E+03
9	6.5748E+30	2.6559E+03	9.0950E+30	2.7534E+03
10	1.7590E+34	2.6578E+03	2.5304E+34	2.7563E+03

MOMENTS ABOUT THE MEAN

1	2.6409E+03	0.	2.7300E+03	0.
2	9.6159E+03	9.8061E+01	1.6086E+04	1.2683E+02
3	3.8537E+05	7.2768E+01	1.4988E+05	5.3116E+01
4	2.8783E+08	1.3025E+02	6.2978E+08	1.5842E+02
5	3.0322E+10	1.2484E+02	5.4653E+09	8.8618E+01
6	1.4779E+13	1.5665E+02	3.4595E+13	1.8051E+02
7	2.4418E+15	1.5785E+02	-4.8364E+14	-1.2525E+02
8	1.0275E+18	1.7843E+02	2.3346E+18	1.9771E+02
9	2.1665E+20	1.8177E+02	-1.4090E+20	-1.7329E+02
10	8.5212E+22	1.9636E+02	1.8514E+23	2.1220E+02

RESULTS FROM RE-BINNING INTO 25 BINS

I	EN	NO.	PSI	+/-
1	2.000E+03	0.	0.	0.
2	2.042E+03	0.	0.	0.
3	2.083E+03	0.	0.	0.
4	2.125E+03	0.	0.	0.
5	2.167E+03	0.	0.	0.
6	2.208E+03	0.	0.	0.
7	2.250E+03	0.	0.	0.
8	2.292E+03	0.	0.	0.
9	2.333E+03	0.	0.	0.
10	2.375E+03	38.	1.121E-23	1.828E-24
11	2.417E+03	89.	2.581E-23	2.732E-24
12	2.458E+03	236.	7.005E-23	4.565E-24
13	2.500E+03	771.	2.955E-22	1.064E-23
14	2.542E+03	1836.	7.340E-22	1.713E-23
15	2.583E+03	3030.	1.114E-21	2.024E-23
16	2.625E+03	4299.	1.288E-21	1.964E-23
17	2.667E+03	5398.	1.304E-21	1.775E-23
18	2.708E+03	5855.	1.082E-21	1.413E-23
19	2.750E+03	4647.	5.859E-22	8.595E-24
20	2.792E+03	4561.	4.015E-22	5.946E-24
21	2.833E+03	4129.	2.528E-22	3.934E-24
22	2.875E+03	3372.	1.410E-22	2.428E-24
23	2.917E+03	2620.	7.490E-23	1.466E-24
24	2.958E+03	1896.	3.300E-23	7.577E-25
25	3.000E+03	2138.	1.360E-23	2.941E-25

....LINE....
REACTION PRODUCT LINE-SHAPE CALCULATION

THIS JOB WAS RUN:		11:29:34	01/29/85 U
USING CODE VERSION LOADED:		12/17/84	18:27:28
RESULTS ARE IN FILES:	OUTX1129		FX105X1129

FRAME 1

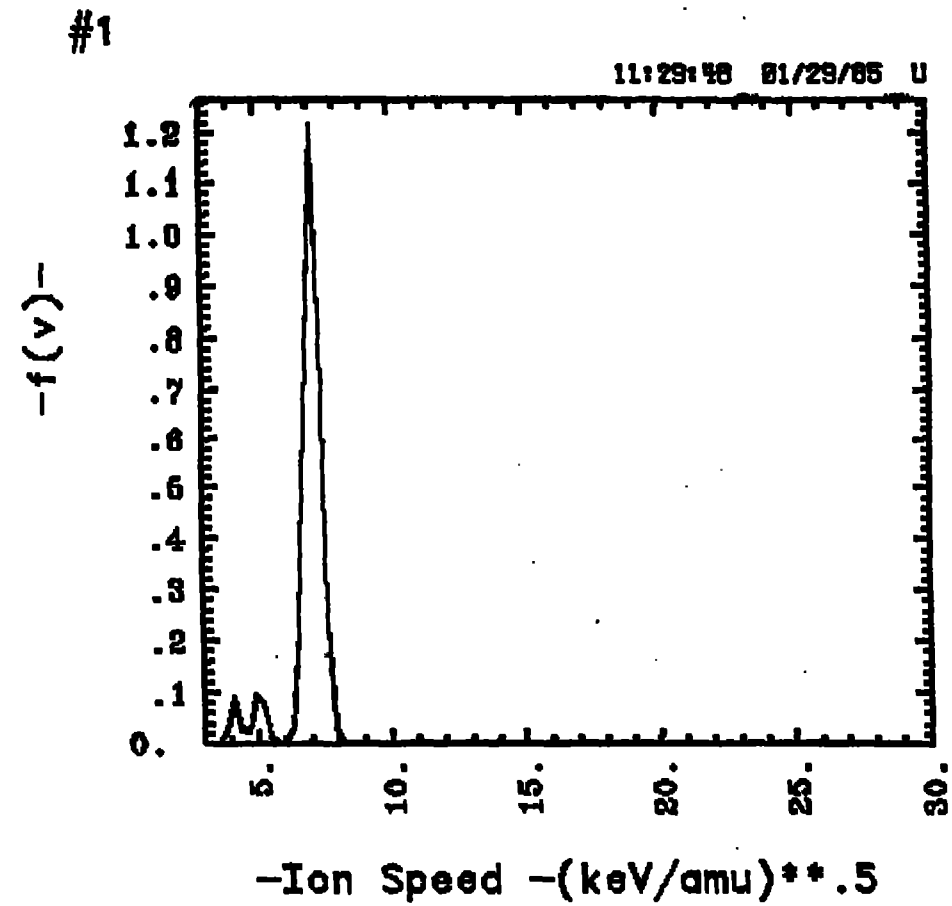

Ion type #1

test problem

FRAME 2

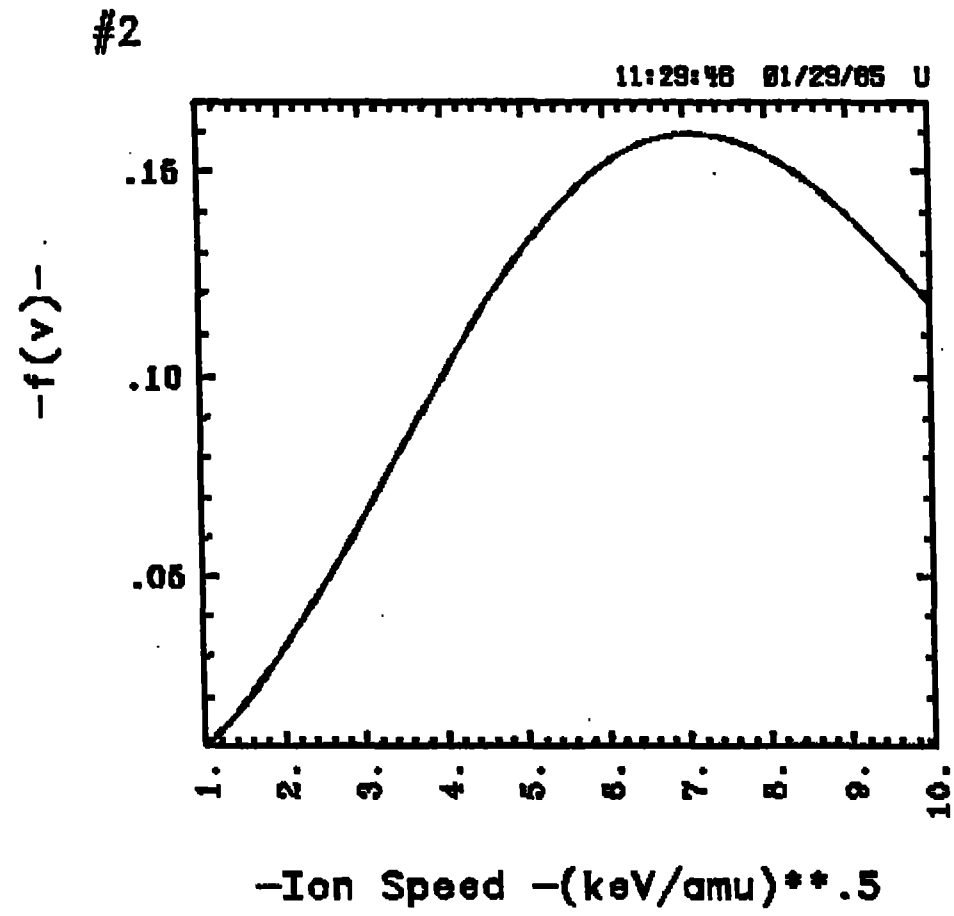

Ion type #2
test problem
FRAME 3

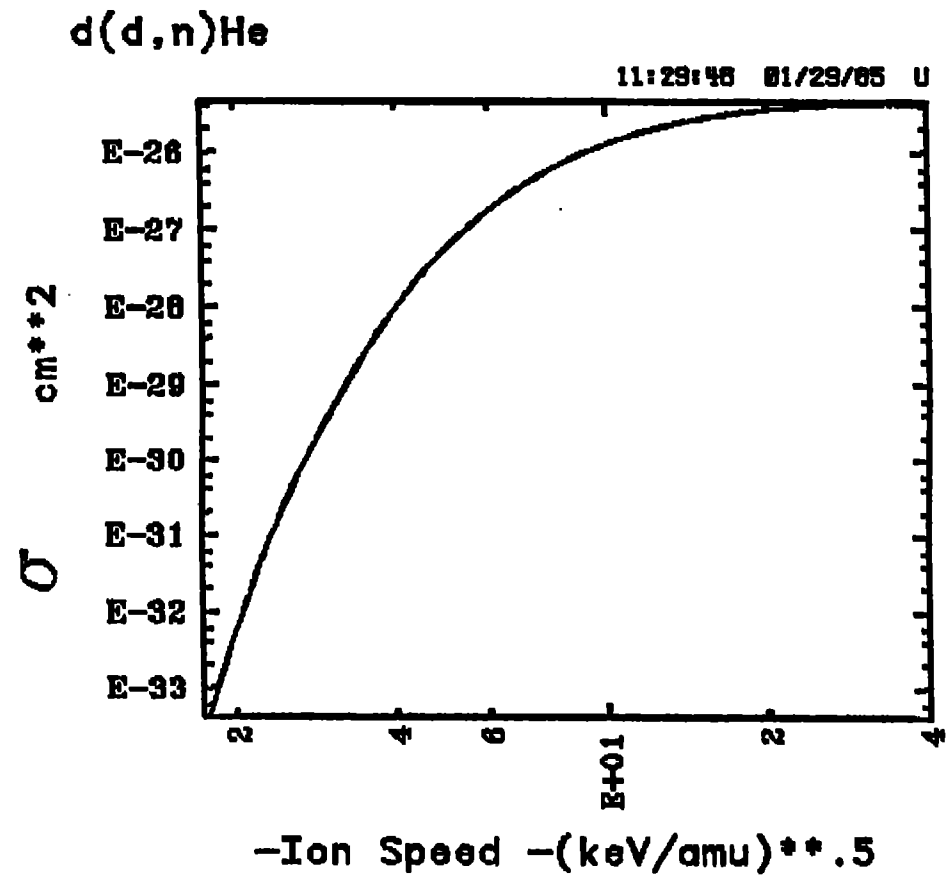

Cross Section
test problem
FRAME 4

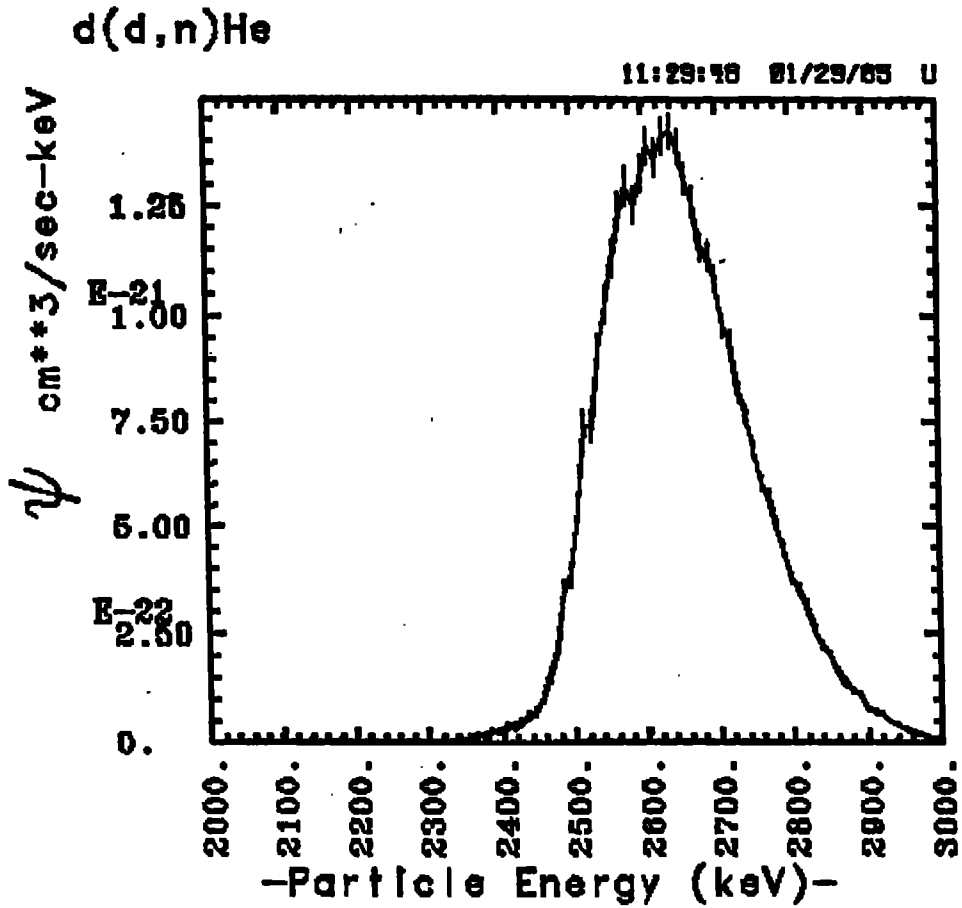

d(d,n)He
test problem
FRAME 5

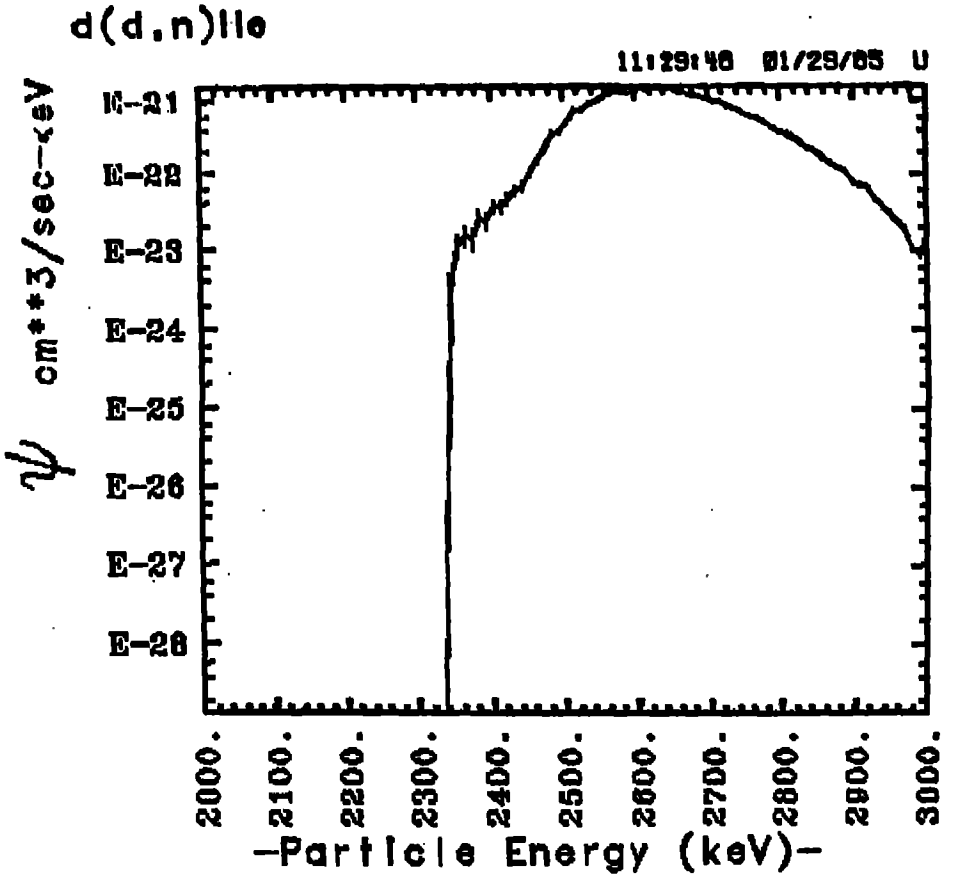

d(d,n)He
test problem
FRAME 6

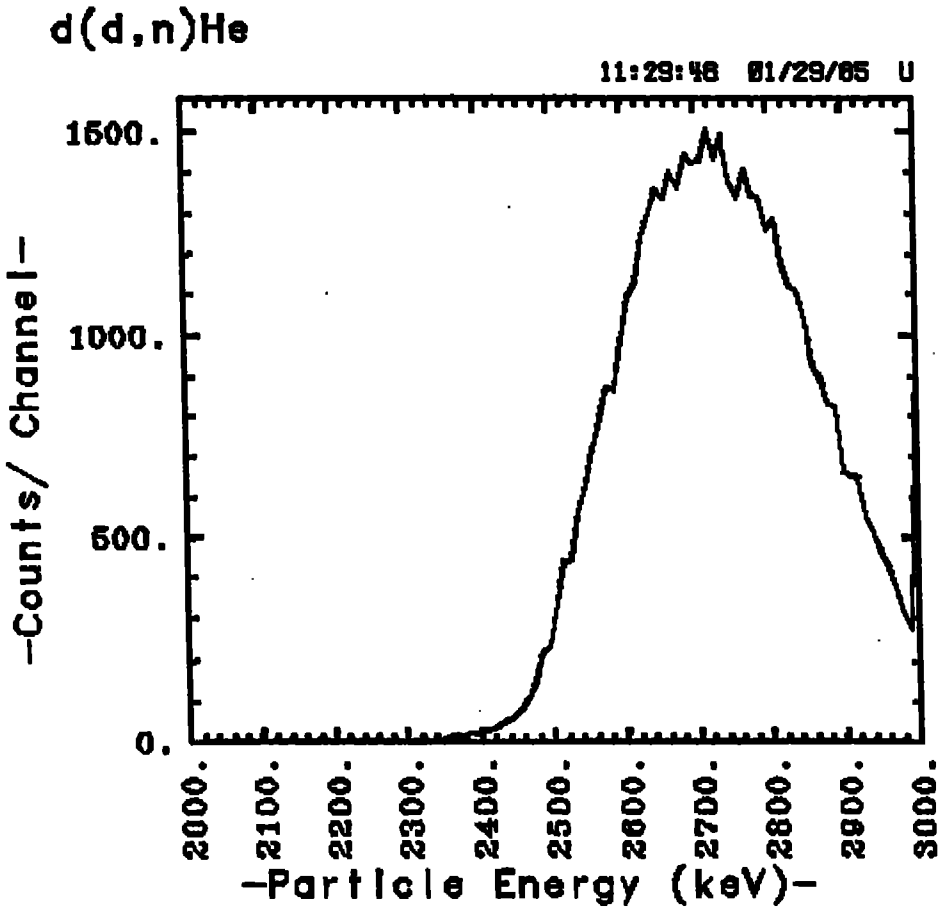

d(d,n)He
test problem
FRAME 7

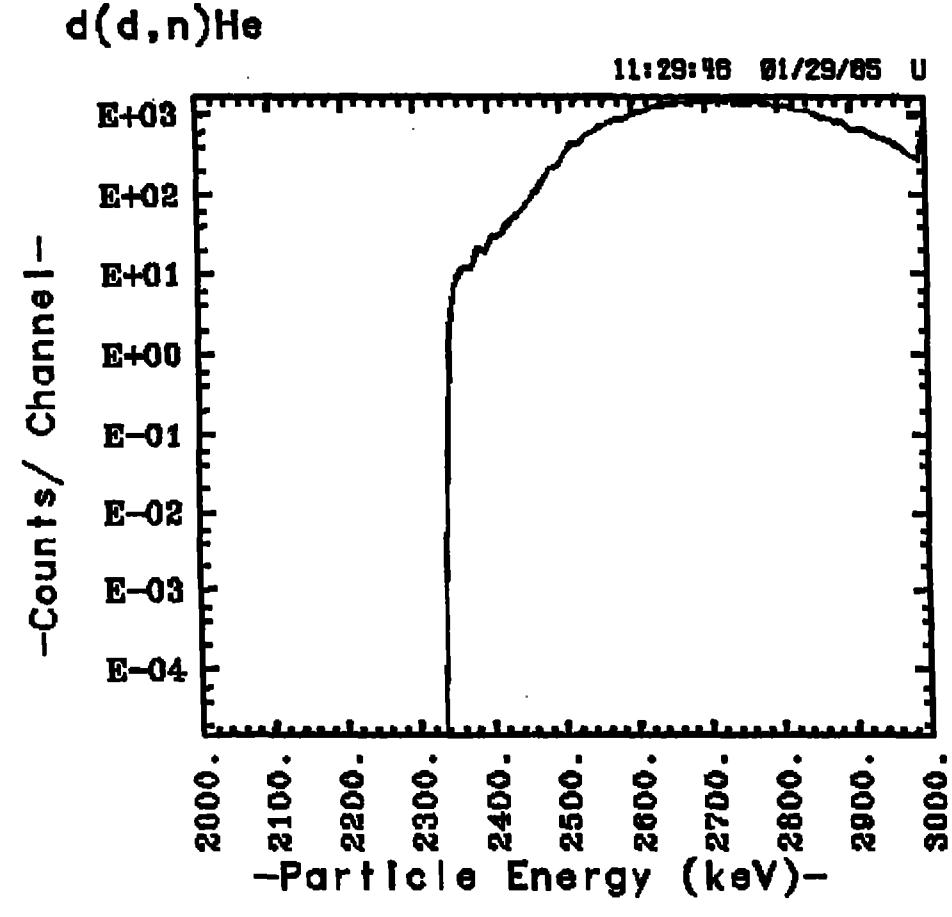

d(d,n)He
test problem
FRAME 8